# Intraband optical absorption in semiconductor coupled quantum dots

Shu-Shen Li and Jian-Bai Xia
*National Laboratory for Superlattices and Microstructures, Institute of Semiconductors, Chinese Academy of Sciences, P.O. Box 912, Beijing 100083, People's Republic of China*
(Received 15 November 1996; revised manuscript received 20 February 1997)

In the framework of effective mass envelope function theory, absorption coefficients are calculated for intraband (intersubband in the conduction band) optical transition in InAs/GaAs coupled quantum dots. In our calculation the microscpic distributon of the strain is taken into account. The absorption in coupled quantum dots is quite different from that of superlattices. In superlattices, the absorption does not exist when the electric vector of light is parallel to the superlattice plane (perpendicular incident). This introduces somewhat of a difficulty in fabricating the infrared detector. In quantum dots, the absorption exists when light incident along any direction, which may be good for fabricating infrared detectors. [S0163-1829(97)02223-6]

## I. INTRODUCTION

Proposals for using optical transitions between quantum confined states for infrared (IR) applications were made in the early days of quantum wells.[1,2] Recently, two collections of papers on intersubband transitions in quantum wells have been published as the result of two NATO Advanced Research Workshops.[3,4] In actual experiments, a superlattice (SL) structure must be employed instead of an isolated quantum well in order to enhance the absorption efficiency. Nojima[5] calculated the absorption coefficients for intraband (intersubband in the conduction band) optical transition in semiconductor SL. The effect of line broadening is taken into account assuming that it comes from the fluctuation of well thickness. Their calculated results well explained the experiments for $In_{0.53}Ga_{0.47}As/In_{0.53}Al_{0.47}$ As SL.[6]

The realization of lateral potentials to form semiconductor quantum dots (QD) has been made possible by a variety of advanced techniques. Xie *et al.*[7] demonstrated a vertically self-organized growth of InAs quantum box islands. A phenomenological model was proposed. The model consistently accounted for the observations, and thus provided clear evidence that the island-induced evolving strain fields provide the driving force for self-assembly or self-organization in island systems. The strong vertically self-organized islands open a new front for studying the novel properties of nanostructures, such as the coupled InAs quantum boxes.

Solomon *et al.*[8] investigated multilayer, vertically coupled, quantum dot structures using layers composed of InAs islands grown by molecular beam epitaxy. They found that the InAs islands were vertically aligned in columns and were pseudomorphic. The electronic coupling between islands increased the photoluminescence linewidth.

Tersoff, Teichert, and Lagally[9] investigated the growth of multilayer arrays of coherently strained islands, which may serve as ''quantum dots'' in electronic devices. A simple model reproduces the observed vertical correlation between islands in successive layers. The structure ''self-organizes'' into a more regular three-dimensional arrangement, providing a possible route to obtain the size uniformity needed for electronic applications of quantum dot arrays.

In Ref. 10, we studied the interband (between conduction band and valance band) optical transition of InAs/GaAs strained coupled quantum dots in the framework of effective mass envelope function theory. In this paper, we will study the intraband (intersubband in the conduction band) optical transition in the structure as same as Ref. 10.

## II. THEORETICAL MODEL

For studying the case of the InAs/GaAs coupled quantum dots, we choose the growth direction (100) as the $Z$ direction of our coordinate system. The InAs dots are periodically arranged boxes. In the $Z$ direction, the width of the InAs dot is $l$, and the distance between two adjacent dots is $d$, the period is then $l+d$. In the parallel direction, the radius of InAs dots is $R$, the distance between two nearly dots is $L-2R$, and $L$ is the period. We choose the boxed region as the unit cell shown in the Fig. 1 of Ref. 10.

According to Burt and Foreman's effective mass theory and taking into account the differences of the effective mass between InAs and GaAs materials,[11,12] the electron envelope function equation is

$$\left[\vec{P}\frac{1}{2m_e^*(x,y,z)}\vec{P}+V_e(x,y,z)\right]F_n(\vec{r})=E_nF_n(\vec{r}), \qquad (1)$$

where $V_e$ and $m_e^*$ are defined by Eqs. (2a) and (2b) of Ref. 10, respectively; $n=0,1,2,\ldots$, denote the ground state, the first excited state, the second excited state, etc. As in Ref. 10, we assume that the electron envelope functions have the following forms:

$$F_n(\vec{r})=\frac{1}{L\sqrt{l+d}}\sum_{n_xn_yn_z} e^n_{n_xn_yn_z} \times e^{[(k_x+n_xK_x)x+(k_y+n_yK_y)y+(k_z+n_zK_z)z]}, \qquad (2)$$

with $k_{ni}=k_i+n_iK_i$, $n_i=0,\pm1,\pm2,\ldots$ $(i=x,y,z)$; $K_x=K_y=2\pi/L$, $K_z=2\pi/(l+d)$. Taking into account the strain, we will calculate the electronic structures and study the intersubband optical transition of the electron. In the effective mass approximation,[13] the matrix element between the two subband states ($\Psi_n$ and $\Psi_0$) in coupled quantum dots can be expressed as follows:

 

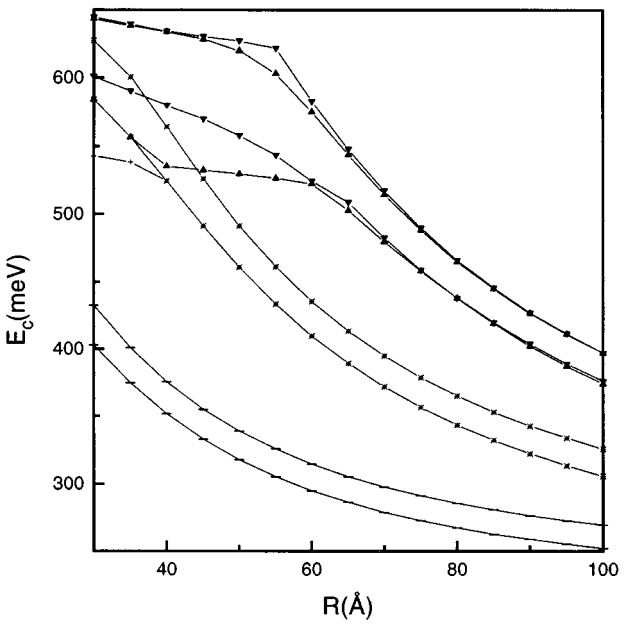


FIG. 1. The conduction subbands and minigaps as a function of QD radius $R$. The two lines marked with same symbols are the bottom and top of corresponding subband, respectively.

$$\langle \Psi_n | H' | \Psi_0 \rangle = \frac{m}{m^*} \langle F_n | H' | F_0 \rangle, \tag{3}$$

where $H'$ is the interaction Hamiltonian between a free electron with mass $m$ and a radiation field. Supposing the angle between the electric vector of light and the growth direction ($Z$ direction) of the QD is $\theta$, and the angle between the electric vector of light and the $X$ direction of the QD is $\beta$. Inserting Eq. (2) into Eq. (3), we obtain

$$\langle F_n | H' | F_0 \rangle = \sum_{n_x n_y n_z} e^n_{n_x n_y n_z} e^0_{n_x n_y n_z} [(k_x + n_x K_x) \sin\theta \cos\beta + (k_y + n_y K_y) \sin\theta \sin\beta + (k_z + n_z K_z) \cos\theta]. \tag{4}$$

Let us focus our attention on the transitions $0 \rightarrow n$ and exclude other possible transitions such as $1 \rightarrow n$, etc. The absorption coefficient is given by

$$\alpha(\hbar\omega) = \frac{8\pi^2 e^2}{\eta c \omega m^2} \sum_n \int \frac{d\vec{k}}{(2\pi)^3} \times |\langle \Psi_n | H' | \Psi_0 \rangle|^2 \cdot \delta(E_n - E_0 - \hbar\omega) \times [f_0(\vec{k}) - f_n(\vec{k})]. \tag{5}$$

In Eq. (5), $\eta$ is the refractive index, and $f_0(\vec{k})$ and $f_n(\vec{k})$ are the occupancy of the electron at the ground state and $n$ excited state, respectively. According to the Fermi distribution function,

$$f_n(\vec{k}) = \frac{1}{e^{[E_n(\vec{k}) - E_F]/K_b T} + 1}, \tag{6}$$

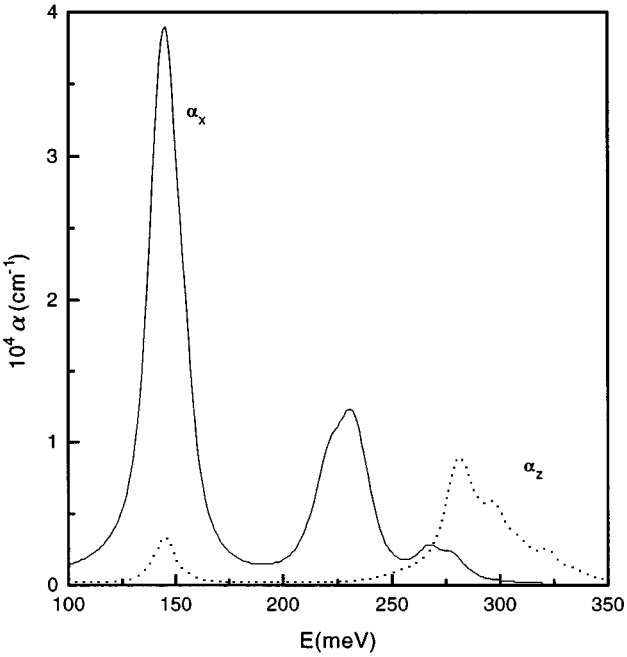


FIG. 2. Absorption coefficient spectra for InAs/GaAs QD at room temperature with $N_{\mathrm{InAs}} = 1.5 \times 10^{18}\ \mathrm{cm}^{-3}$ and $L = 200$ Å, $R = 50$ Å, $l = 30$ Å, and $d = 50$ Å. The solid and dotted lines are the results for electric vector of incident light perpendicular to the growth direction ($\theta = \pi/2$, and $\beta = 0$) and parallel to the growth direction ($\theta = 0$), respectively. The latter has been multiplied by 10.

where $E_F$ is the Fermi energy of electron. For a given electron concentration ($N$), $E_F$ can be determined using the standard expression

$$N = 2 \int_{\mathrm{BZ}} \sum_n f_n(\vec{k}) d\vec{k} / (2\pi)^3. \tag{7}$$

In order to obtain a smooth absorption spectrum, we replace the $\delta$ function in Eq. (5) with a Lorentzian function with a half-width $\Gamma$, viz.,

$$\delta(E - \hbar\omega) \approx \frac{\Gamma}{\pi[(E - \hbar\omega)^2 + \Gamma^2]}. \tag{8}$$

The magnitude of $\Gamma$ is roughly equal to the energy spacing of the eigenstates.

## III. RESULTS AND DISCUSSION

In the dot material, the compressive stress alters the curvature of the bulk bands causing the effective masses to differ from those of unstrained InAs. As same Ref. 15, we used the effective masses of bulk InAs under the average hydrostatic strain present in the dot material. In the conduction band, the calculations yield effective mass $0.04 m_0$ for strained InAs .

To validate our results on the optical constants, we give the conduction subbands and minigaps as a function of QD radius $R$ in Fig. 1 for $L = 100$ Å $+ 2R$, $l = 30$ Å, and $d = 50$ Å. Two lines marked with the same symbols are the bottom and top of the corresponding subband, respectively.

We take the material parameters as in Ref. 10, room temperature $T = 300$ K, refractive index $\eta = 3.5$,[14] $N_{\mathrm{InAs}} = 1.5 \times 10^{18}\ \mathrm{cm}^{-3}$, and $N_{\mathrm{GaAs}} = 0$. The electron concentration $N$ can be determined by

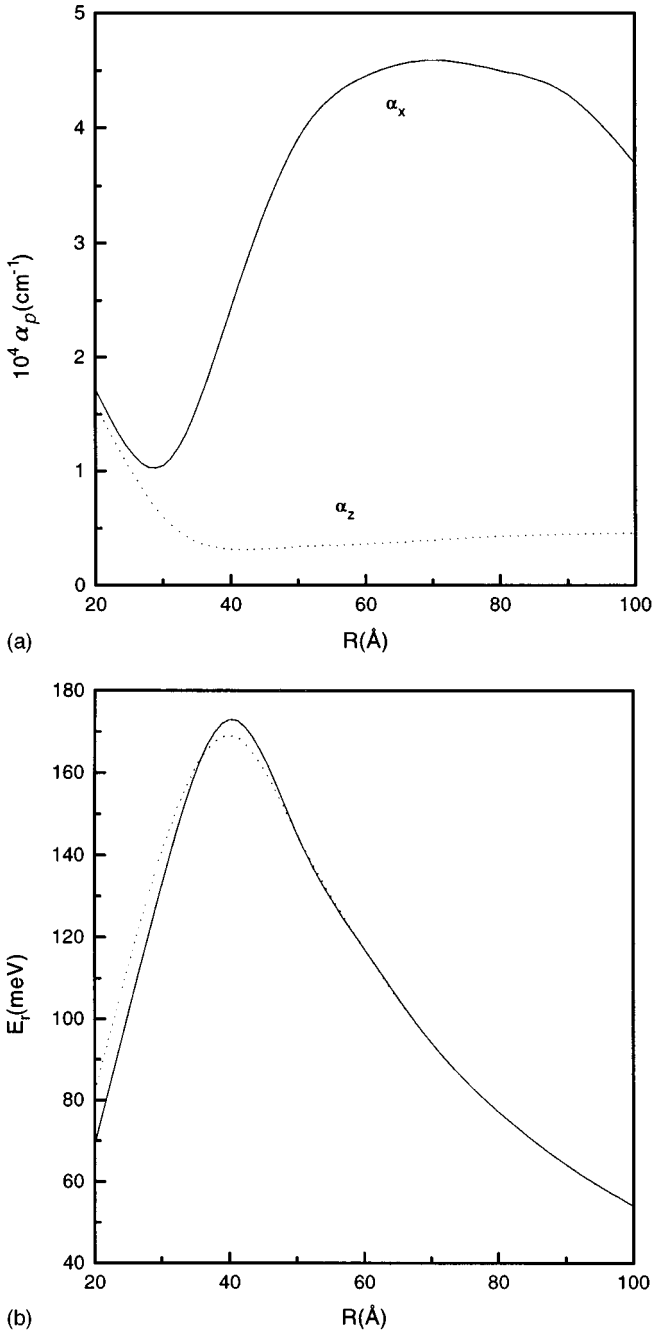


FIG. 3. (a) Maximum absorption coefficient and (b) resonance energy as a function of $R$ for the $0\rightarrow1$ transition in InAs/GaAs QD at room temperature with $N_{\mathrm{InAs}}=1.5\times10^{18}\,\mathrm{cm}^{-3}$ and $L=200$ Å, $l=30$ Å, and $d=50$ Å. The solid and dotted lines are the results of electric vector of incident light perpendicular to the growth direction ($\theta=\pi/2$, and $\beta=0$) and parallel to the growth direction ($\theta=0$), respectively.

$$N=\frac{\pi R^2 l}{L^2(l+d)}N_{\mathrm{InAs}}. \tag{9}$$

Figure 2 gives the absorption coefficient spectra for $L=200$ Å, $R=50$ Å, $l=30$ Å, and $d=50$ Å. The solid and dotted lines are the results for the electric vector of incident light perpendicular to the growth direction ($\theta=\pi/2$, and $\beta=0$) and parallel to the growth direction ($\theta=0$), respectively. Our calculated results show that the absorption coefficient is weakly dependent on $\beta$. From Fig. 1, we can find that the absorption coefficient for the electric vector perpendicular to the growth direction is larger than that for the electric vector parallel to the growth direction. This result is very different from the case of SL. In SL, the absorption coefficient is always zero when the electric vector of incident light is perpendicular to the growth direction. We think that it may be more convenient to fabricate an infrared detector using a QD device rather than using a SL device. The energy band of the ground and the first excited states has a small width due to the small coupling between dots. So, the resonance energy of the $0\rightarrow1$ transition is almost located at the same site when changing the directions of incident light.

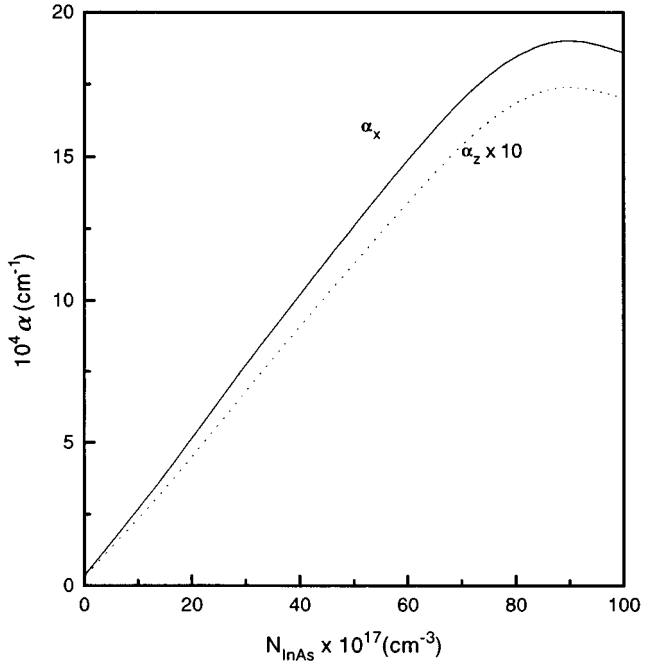


FIG. 4. Maximum absorption coefficient as a function of electron concentration $N_{\mathrm{InAs}}$ for the $0\rightarrow1$ transition in InAs/GaAs QD at room temperature with $L=200$ Å, $R=50$ Å, $l=30$ Å, and $d=50$ Å. The meaning of solid and dotted lines are the same as in Fig. 1.

Figures 3(a) and 3(b) show maximum absorption coefficient $\alpha_p$ and resonance energy $E_r$ as a function of QD radius $R$ for the $0\rightarrow1$ transition at room temperature with $N_{\mathrm{InAs}}=1.5\times10^{18}\mathrm{cm}^{-3}$ and $L=100$ Å$+2R$, $l=30$ Å, and $d=50$ Å. The solid and dotted lines are the results for electric vector of incident light perpendicular to the growth direction ($\theta=\pi/2$, and $\beta=0$) and parallel to the growth direction ($\theta=0$), respectively. The $\alpha_p$ value decreases and the $E_r$ value increases with decreasing $R$ (from 80 Å) and deviate from the trend at a critical radius $R_c$. When $R$ is smaller than $R_C$, the first excited state will exceed the potential barrier height, and the energy band of the first excited state becomes broad. So, the $\alpha_p$ value will increase and the $E_r$ value will decrease with decreasing $R$ when $R$ is smaller than $R_C$. From Fig. 3(a), we can find that the maximum absorption coefficient is basically constant when the electric vector of the incident light is parallel to the growth direction ($\theta=0$). This is due to the constant width of the QD along the growth direction.

Figure 4 shows the maximum absorption coefficient $\alpha_p$ of the $0 \rightarrow 1$ transition at room temperature for the same QD material parameters as in Fig. 2 as a function of electron concentration ($N_{\mathrm{InAs}}$). The meaning of the solid and dotted lines is the same as in Fig. 2. From this figure we can find that the $\alpha_p$ values increase with increasing $N$ and deviate from the line at higher $N$ values. This deviation is thought to imply the onset of occupation by electrons of the first excited state to which the transition from the ground state should occur. The critical $N$ value for this deviation approximately coincides with the value at which the Fermi function goes into the first excited state to some extent. This characteristic is the same as the results of SL.

## IV. SUMMARY

In this paper, we have studied the intraband (intersubband in the conduction band) optical transition of InAs/GaAs coupled quantum dots in the framework of effective mass envelope function theory. The absorption coefficient and resonance energy as a function of QD radius and the absorption coefficient as a function of electron concentration have been calculated. The calculated results show that the intraband absorption in coupled quantum dots is quite different from that in superlattices. In superlattices, the absorption does not exist when the electric vector of light is parallel to the superlattice plane (perpendicular incident). This introduces somewhat of a difficulty in fabricating the infrared detector. In quantum dots, the absorption exists when light is incident along any direction, which may be good for fabricating infrared detectors.

## ACKNOWLEDGMENT

This work was supported by the National Natural Science Foundation of China.

[1] L. L. Chang, L. Esaki, and G. A. Sai-Halaz, IBM Tech. Disc. Bull. **20**, 2019 (1977).
[2] L. Esaki and H. Sakaki, IBM Tech. Disc. Bull. **20**, 2456 (1977).
[3] *Intersubband Transitions in Quantum Wells*, edited by E. Rosencher, B. Vinter, and B. Levine (Plenum, New York, 1992).
[4] *Quantum Well Intersubband Transition Physics and Devices*, edited by H. C. Liu, B.F. Levine, and J. F. Andersson (Kluwer, Dordrecht, 1994).
[5] S. Nojima, Phys. Rev. B **41**, 10 214 (1990).
[6] B.F. Levine, A. Y. Cho, J. Walker, R. J. Malik, D. A. Kleinman, and D. L. Sivco, Appl. Phys. Lett. **52**, 1418 (1988).
[7] Q. Xie, A. Madhukar, P. Chen, and N. P. Kobayashi, Phys. Rev. Lett. **75**, 2542 (1995).
[8] G. S. Solomon, J. A. Trezza, A. F. Marshall, and J. S. Harris, Jr., Phys. Rev. Lett. **76**, 952 (1996).
[9] J. Tersoff, C. Teichert, and M. G. Lagally, Phys. Rev. Lett. **76**, 1675 (1996).
[10] Shu-Shen Li, Jian-Bai Xia, Z. L. Yuan, Z. Y. Xu, Weikun Ge, Xing Rong Wang, Y. Wang, J. Wang, and L. L. Chang, Phys. Rev. B **54**, 11 575 (1996).
[11] M. G. Burt, J. Phys. Condens. Matter **4**, 6651 (1992).
[12] B. A. Foreman, Phys. Rev. B **52**, 12 241 (1995).
[13] J. M. Luttinger and W. Kohn, Phys. Rev. **97**, 869 (1955).
[14] *Semiconductors. Physics of Group IV Elements and III-V Compounds*, edited by K.-H. Hellwege and O. Madelung, Landolt-Bornstein, New Series, Group III, Vol. 17, Pt. a (Springer-Verlag, Berlin 1982).
[15] M. A. Cusack, P. R. Briddon, and M. Jaros, Phys. Rev. B **54**, R2300 (1996).